5th International Chemical Engineering Congress and Exhibition
Kish Island, 2 - 5 January 2008

Two Dimensional numerical simulation of turbulent flow in a mixing layer using Transport Element Method

N. Ghiasi Tabari [1*], **Gh. Heidarinejad** [2]
1-PhD Student of mechanical engineering, Tarbiat Modares University
2-Associate Professor, mechanical engineering, Tarbiat Modares University

ABSTRACT

Mixing process is one of the most important phenomena in engineering science. Turbulent effect and oscillations in the base flow increase the mixing rate noticeably. In this research a non-reacting concentration field in a mixing layer is simulated for high Reynolds number by solving the scalar transport equations. We used a grid free CFD scheme named Transport Element method in order to model the concentration field in a lagrangian frame. The concentration gradient is calculated in vortex structures and other cross sections in the field. Also mean concentration profile and concentration fluctuation diagram are obtained for various diffusion coefficients. The results are in good agreement with other experimental data.

Key word: Concentration field, Mixing layer, Turbulent flow, Transport Element method, Grid free technique, Lagrangian frame

INTRODUCTION

The mixing phenomena is widely happening in industry mostly in chemical reactors, mixers and pipe lines. Moreover for study of combustion the mixing procedure of air-reactants should be well studied first. Non-premixed turbulent flow in a shear layer has been the subject of extensive experimental, theoretical and numerical investigations. Because of the unstable nature of mixing layer, the two fluid flow can be mixed efficiently. Grinstein et al.[1] used a flux-corrected transport scheme to simulate the development of coherent structures in a 2D spatially-evolving shear layer and examined their effect on mixing. Beale & Majda [2] also used a class of lagrangian particle methods to solve the Euler equation for a 2D incompressible flow; the method is based on the discretization of the vorticity into finite vortex elements which carry radially-symmetric, compact support of vorticity. Ghoniem & Givi [3] used a vortex/transport element method to investigate the evolution of a spatially-growing constant density mixing layer using a low heat release chemical reaction. Souterio [4] also simulated the mixing layer with variable density. Heidarinejad [5] also used TEM to simulate high Reynolds reacting shear layer. He investigate the Reynolds number effect on the mixing rate.

Vortex methods or Transport Element method have significant advantages for numerical simulations of separated flows:

1. In vortex methods, only small portion of the flow region where vorticity occurs, need to be described [6].
2. Lacking fix grid, vortex methods can easily handle flows around complicated geometries and can avoid significant numerical dissipation.
3. The turbulent flow simulation does not need any turbulence modeling [7].
4. Applying curl operator on the momentum equation, pressure term eliminates from equations.

* *Nima_ghiasi_te@yahoo.co.uk*

5. In external flows, vortex methods can treat boundary conditions without restricting the computational domain to a finite zone.
6. In the computation of the velocity field from the vorticity, mass conservation can be satisfied exactly.

Recent advances in developing fast adaptive vortex methods and the parallel implementation of vortex algorithms on computers cluster have removed many limitations on the number of vortex elements that will be reasonably applied in complex and high Reynolds number flow simulations.

In this paper we will mainly present a direct mesh-less method without using turbulence modeling to simulate a spatial mixing layer.

METHOD DISCRIBTION AND GEOMETRY

In common random vortex method the vorticity instead of velocity is used as an unknown parameter in equations. In extended Transport Element method the scalar gradient instead of scalar could be used as an unknown in the same way. It is because that in most fluid flows particularly in shear layers only the small portion of flow is covered by the scalar gradient rather than scalar itself; so using scalar gradient as an unknown in equations is more efficient. (note that in our work "concentration" is the desired scalar we are discussing about). As the flow map usually encounters sever stretch and distortion; in order to reduce the numerical error, we used a conservative Transport Element method to calculate the exact value of concentration in the field. In this method it is proven that the stretching rate and distortion of the iso-scalar lines is proportional to scalar gradient directly (Fig. 1).

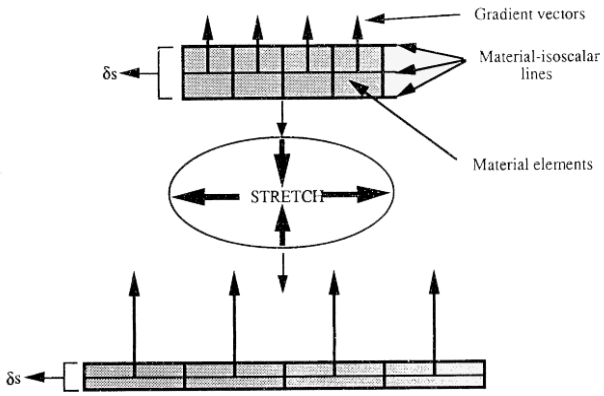

Fig(1): The relation between stretching rate of iso-scalar lines and scalar gradient

The geometry of the problem (Fig. 2) is made of two parallel sheet having one unit width and variable length. Two flows enter the channel from top and bottom of an splitter in the middle of channel at the inlet section. The upper fluid velocity is more than the other in the bottom. The inlet concentration profile for flow is given by an error function in which the concentration of the upper and the lower flow is considered zero and unity respectively. The walls are considered impermeable and since the Reynolds number is high, the growth of the boundary layers on the confining walls is neglected. The computational elements are deleted at the exit plane. This introduces a perturbation upstream and ensures that the roll up and at least the first pairing will take place within the domain. Since this perturbation is not applied in an organized manner, the resulting shear layer will be considered as an unforced layer. Also the potential scalar component for the satisfaction of boundary condition is imposed. This potential component is derived from schowarz – christoefell transformation to map the two-dimensional physical plane onto the upper-half-plane of the computational domain using:

$$F(x) = p\ (x - \frac{1}{x}) \qquad (1)$$

In the mapping the two incoming streams are represented by two line sources with the strength of $S_1 = 0.5U_1/p$ and $S_2 = 0.5U_2/p$ located at $x_{s1} = (-1,0)$ and $x_{s2} = (+1,0)$, respectively (Fig. 3). Note that 0.5 in the expression of the strength comes from the fact that these sources cover only the upper half of the computational plane.

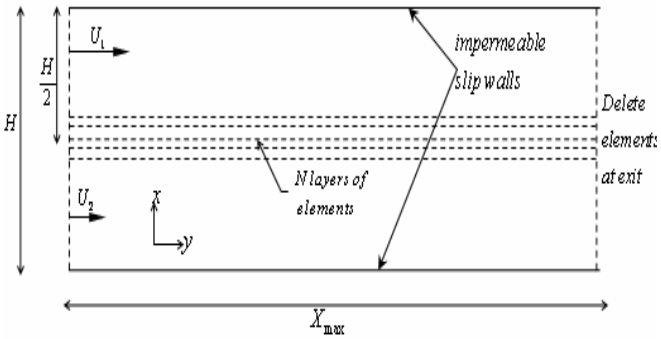

Fig(2): Schematic of the geometry

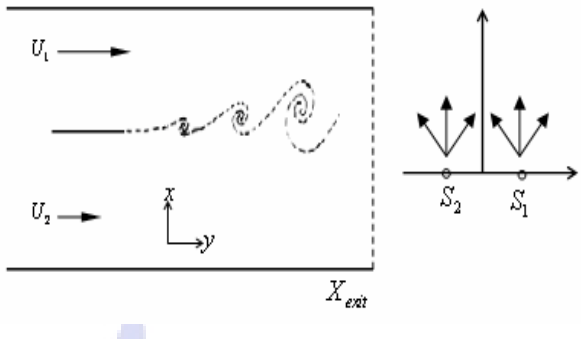

Fig(3): Physical and computational domain

FIELD EQUATIONS

The governing equations in lagrangian framework are presented below:

$$\frac{d\mathbf{g}}{dt} = -\mathbf{g}.\nabla\mathbf{u} - \mathbf{g}\times w + \frac{1}{Ne}\nabla^2\mathbf{g} \quad (2)$$

$$s(\mathbf{x}) = \int \nabla G(\mathbf{x}-\mathbf{x}')\cdot\mathbf{g}(\mathbf{x}')d\mathbf{x}' + s_p(\mathbf{x}) \quad (3)$$

$$s(\mathbf{x},t) = \sum_{i=1}^{N}\Delta\mathbf{g}_i(t)\cdot\frac{(\mathbf{x}-\mathbf{x}_i)\cdot(\mathbf{y}-\mathbf{y}_i)}{r_i^2}K(r_i) \quad (4)$$

$$d^2 = d_0^2 + 4a\,t \quad (5)$$

The equation (2) is first split into two individual equations in each time step as the fractional step rule. Then the equation (4) is used for the calculation of concentration value at the center each element. After which the diffusion effect is simulated by spreading the core size according to the equation (5).

RESULTS AND DISCUSSION

The results are obtained under following conditions:

Duct length: $D_L = 10.5$

Duct height: $D_H = 1$

Time step: $\Delta t = 0.01$

Velocity ratio: $U_1/U_2 = 2$

Results are taken for various Peclet numbers in order to show the effect of molecular diffusion in mixing dynamics. In our calculation the Pr number is considered unity so the Reynolds number and Peclet number are the same. According to the mentioned conditions, the development of mixing layers downstream of a splitter plate which is initially dominated by a linear instability mechanism is sketched in Fig. 4 for the Reynolds number: 2×10^3. The initial vorticity distribution is unstable to small perturbations via the Kelvin-Helmholtz instability mechanism because of the velocity gradient between two layers. Thus, two-dimensional waves grow with downstream distance and rollup of vortices are observed.

Fig. 5 shows the instantaneous profiles of the concentration at different sections down-stream the channel superimposed on the instantaneous distribution of the vortex, or transport elements for viscous calculation. The sections are chosen at the centers of the vortex eddies. The distributions show that even at sections far down-stream of the splitter plate, zones of completely unmixed fluid still exists within the layer (unmixed-ness). These zones correspond to the gulfs or "tongues" of pure fluid brought into the layer from either side by the inviscid

mechanism of entrainment, i.e. , the convective transport of fluid across the centerline of the layer by the roll up of the vorticity field.

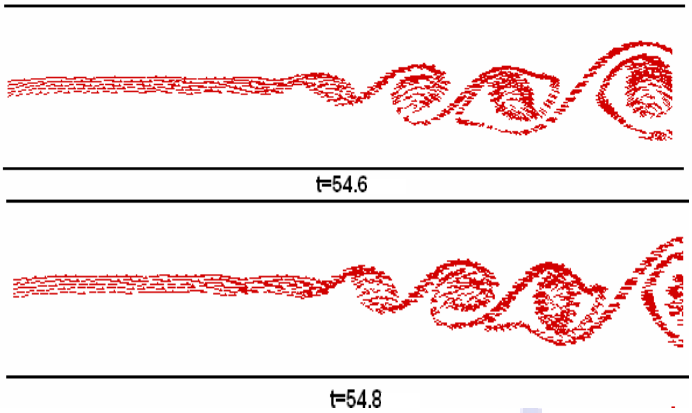

Fig(4): The schematic of spatial shear layer in two different non-dimensional times

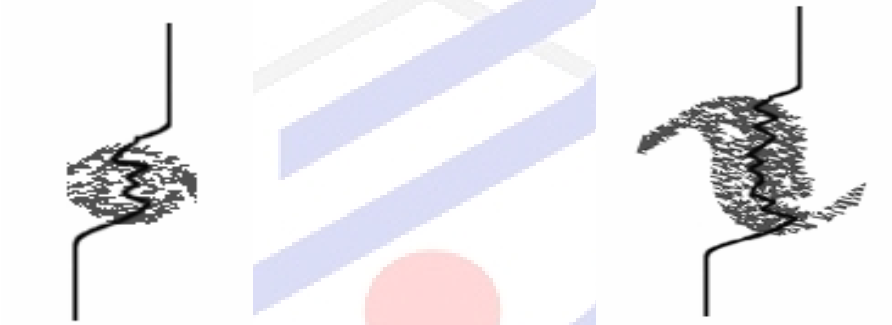

X=1.60 X=4.05

Fig(5): Instantaneous concentration profile across the mid-section of the eddies

Instantaneous concentration profiles show clear signs of asymmetric entrainment within the large structures. Mixing asymmetry which arises due to the asymmetric growth of the eddies during the initial stages of roll up, is indicated by the fact that the profiles are not symmetric around the centerline. Thus, asymmetric entrainment is due to the asymmetric flow field generated by unequal free stream velocities on the two sides of the layer and by the down-stream growth of the vorticity concentration in the cross-stream direction in the spatially-growing layer. We also learn from Fig. 5 that the average concentration of the scalar in the fluid within the eddy is less than the mean average of the concentration on the two streams. The fluid trapped within the eddy is defined by concentration ($0 < c < 1$), but not equal to neither 0 nor 1. The average value of the concentration within the eddy is known as the preferred mixture fraction c_p; since $c_p < 0.5$, because the eddy entrains more fluid from the high-speed stream where $0 < c < 0.5$ than from the low-speed stream where $0.5 < c < 1$.

The concentration profile at the upstream before the roll up of eddies and in the downstream before pairing are shown in Fig. 6; as it is clear in this cross-section (across the braids) because of stretching of the layers and due to large gradients, there exist few elements and a narrow braid is formed; so because of this reason, a sharp scalar gradient can be detected there.

X=4.65 X=0.6

Fig(6): Instantaneous concentration profile across the braids

In order to validate our scheme, we compare the numerical results with the experimental measurements of Masutani & Bowman [8]. This experiment was selected for comparison because the two-dimensionality of the flow was carefully maintained and verified and hence it provides experimental measurements of mixing statistics. In Fig. 7, we plot the averaged concentration profiles for different values of the Peclet number at the stream-wise location of x=5 and Fig. 8 at different stream-wise location for the Peclet number equal to 2500, both compared with the data of Masutani & Bowman.

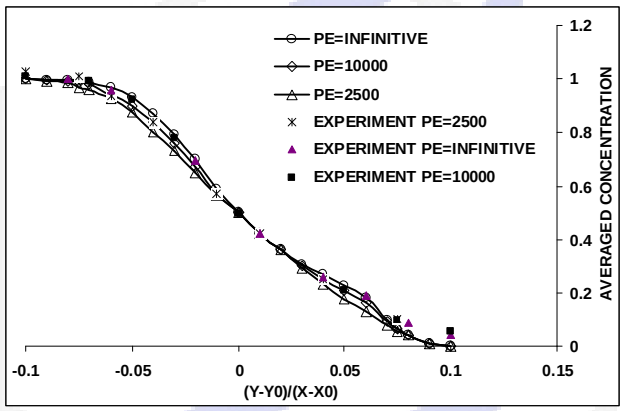

Fig(7): Time-averaged concentration profile at x=5 for different Peclet numbers, comparison with Ref [8]

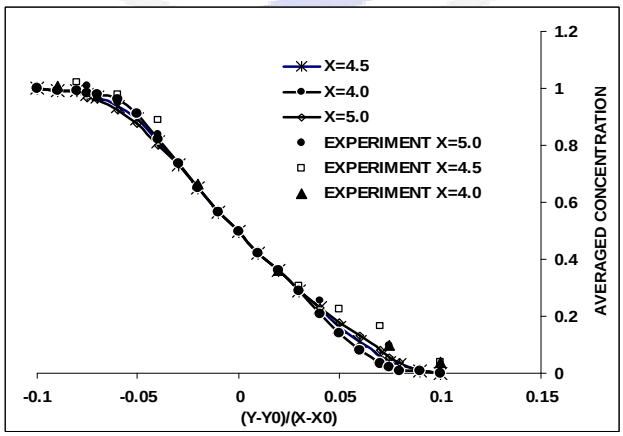

Fig(8): Time-averaged concentration profile for different cross-sections and Pe=2500, comparison with Ref [8]

The mean concentration profiles differ substantially from the initial error function profile, and develop down-stream to form a zone of almost constant value, between two inflection points, around the midsection of the shear layer and toward the high-speed side. Diffusion, which generates strong fluxes around areas of sharp gradients, tends to make the profile smoother. However, as shown by Fig. 7, the effect of diffusion on the mean concentration is minor.

This supports the hypothesis that, in these shear flows, mixing is entrainment-dominant and the entrainment, while it is a consequence of the vorticity-induced field, acts on the vorticity-free part of the flow by Biot-Savart effect. Mixing enhancement by the roll up of the shear layer, due to its intrinsic instability, is thus not limited to the neighborhood of the area where $|w| \neq 0$. Instead the mixing zone extends further into the free streams as we move downstream.

The root-mean-squared concentrations fluctuations are shown in Fig. 9 for different values of the Peclet number at the same stream-wise location; and Fig. 10 at different stream-wise locations for the same Peclet number, both compared with the experimental measurements of Masutani & Bowman. As expected, at zero molecular diffusion the maximum value of c' approaches 0.5, the unmixed state, indicating that the concentration in the fluid passing by the measurement point is altering between the two extreme states. With increasing the level of molecular diffusion, the maximum value of c' decreases and the whole profile attains smaller values showing that the limits between which the value of c is oscillating decrease. The peak and the wide plateau which are observed in this distribution correspond roughly to the transition between the slow stream in which $c = 1$ and the mixing core of the eddy.

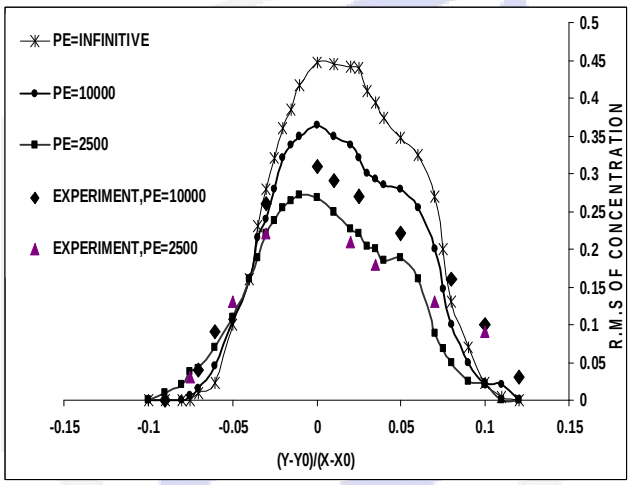

Fig(9): Time-averaged concentration fluctuations at x=5 for different Peclet numbers, comparison with Ref [8]

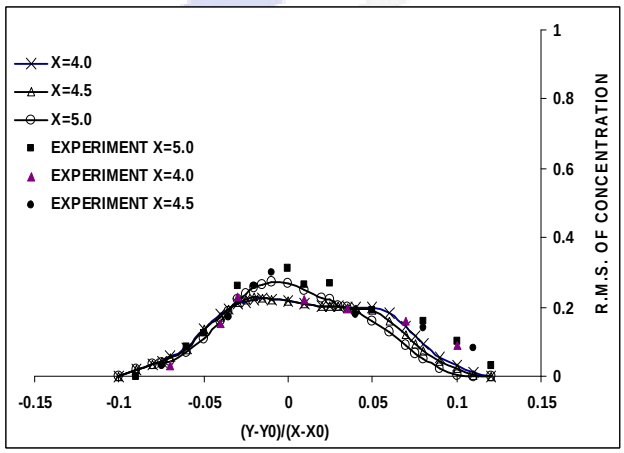

Fig(10): Time-averaged concentration fluctuations for different cross-sections and Pe=2500, comparison with Ref [8]

Fig.9 shows that molecular diffusion has a pronounced effect on the concentration fluctuations, emphasizing the influence of diffusion on the instantaneous profiles and on the outcome of time-dependent process which may take place within the shear layer, such as chemical reactions. Fig. 10 shows that concentration fluctuations reach self-similarity

downstream of the station at which the mean profiles reach self-similarity, similar to the velocity profiles. This is not surprising since the controlling transport mechanism here is convection. The figure also shows that the penetration of the transported species con not be measured by its mean values only. Some deviations between the numerical results and the experimental measurements, which may have resulted in different growth rates, may be attributed to the relative amplitude of noise in the numerical and experimental studies, and the expected scatter in experimental results.

In Fig. 11 and Fig. 12 the mean concentration profile and the root-mean-square concentration fluctuation at the stream-wise cross-section (x=5 & Pe=2500) is compared with another numerical result based on F.D method in ref [9] and Masutani & Bowman's experimental results. As a consequent, the present results are in a better agreement with experimental data; also it can be understood from Fig. 12 that the maximum value for c' is less than the $k-e$ model prediction, so the mixing is well done in our present work.

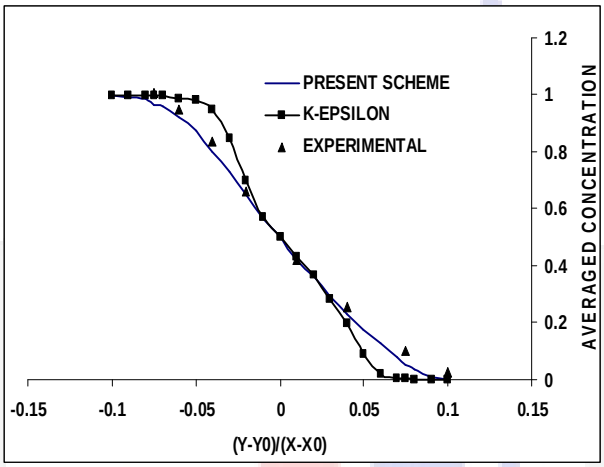

Fig(11): Time-averaged concentration profile at x=5 for Pe=2500 compared with other numerical method

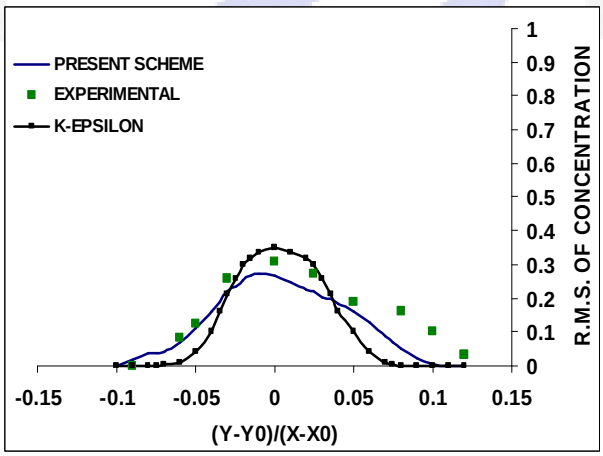

Fig(12): Time-averaged concentration fluctuations at x=5 for Pe=2500 compared with other numerical method

CONCLUSIONS

Numerical simulation of a non-reacting, uniform density, spatially-growing, confined two-dimensional shear layer has been performed using a transport element method. Some remarkable results obtained from the present study are:

1- The results show that the basic dynamical processes that govern the development of a shear layer are the roll up of the initial vorticity layer into large scale eddies after an

initial delay during which perturbations are selectively amplified, and the pairing of these eddies downstream.

2- We found that the velocity difference across the layer leads to mixing asymmetry within the large structure since the layer is forced to entrain more high-speed fluid than low-speed fluid. These unequal entrainment fluxes are induced by an un-symmetric large vortex eddy which forms under the influence of conditions imposed by a non-uniform field governed by the boundary condition. This asymmetry offers a passive means of controlling the mixing within the layer by exchanging the scalars between the two streams.

3- The statistics of the numerical results show good agreement with the experimental measurements within the nonlinear range. These statistics are generated solely by intrinsic instability of the shear layer, which leads to the generation of flow unsteadiness downstream of steady boundary conditions. The statistics of the passive scalar emphasize the important role of molecular diffusion in the mixing process and indicate that a mean preferred mixture fraction, which is different from the average mean of the two streams, exits within the eddies.

NOMENCIATURE

s	Non-reacting Scalar
$\mathbf{g}$	Scalar gradient
G	Green function
$K(r_i)$	Kernel function
Ne	Peclet number×Lewis number
d	Core radius

REFERENCES

1- Grinstein, F.F , Oran, J.P., "Numerical simulations of asymmetric mixing in Planer shear flows ", *J. Fluid Mech* . , Vol. 165,1986 , PP. 201-220.

2- Beale,J.T. and Majda , A., "Vortex Methods . II: Higher order accuracy in two and three dimensions ", *Math. of Comp*., Vol. 39 ,No.159 ,1982 , PP. 29-52.

3- Ghoniem, A.F. and Givi, P., "Lagrangian simulation of a reacting mixing layer at low heat reaease", *AIAA Journal* Vol. 26 ,No. 6, 1988 , PP. 690-697.

4- Soteriou. M.C., "Numerical study of turbulent combustion in a shear layer" , *PhD Thesis Massachusets Institute of Technology (MIT)*, 1991.

5- Heidarinejad G., "Vortex simulation of the reacting shear layer", *PhD Thesis, Massachusets Institute of Technology (MIT)*, 1989.

6- Sebastien Rouvreau, "Two-dimensional viscous vortex flow around a circular cylinder", *Aerosp.Sci.Technol*, 85-94, 5(2001).

7- Ghoniem, A .F. and Ng, K. K., "Numerical study of a dynamics of a forced shear layer", *Journal of Computational Physics*, vol. 30, pp. 706-721, 1987.

8- Masutani, S.M, Bowman, C.T, "The structure of a chemically reacting plane mixing layer", *J. Fluid Mech*, Vol. 172, 1986, PP 93-126.

9- Yang, W. B., "$k-e$ simulation of mixing layer", *Journal of Computational and Applied Mathematics*, 163, pp. 311–318, 2004.